

## 3D characterisation of the structure of activated carbon packed beds using X-ray microtomography

M. C. Almazán-Almazán<sup>1</sup>, A. Léonard<sup>2</sup>, J. López-Garzón<sup>1</sup>, J. Abdullah<sup>3</sup>, P. Marchot<sup>2</sup>, S. Blacher<sup>2</sup>

<sup>1</sup> Department of Inorganic Chemistry, University of Granada, Fuentenueva s/n, Granada, Spain

<sup>2</sup> Laboratory of Chemical Engineering, University of Liège, Sart-Tilman, Belgium –

[A.Leonard@ulg.ac.be](mailto:A.Leonard@ulg.ac.be)

<sup>3</sup> Centre for Computed Tomography and Industrial Imaging, Malaysian Nuclear Agency, Bangi, 43000 Kajang, Malaysia

### ABSTRACT

*When using carbons grains as adsorbent, the 3D bed pore structure can have a large impact on the operation of the filter, through the modification of the transport properties inside the bed. In order to gain insight into the relation between morphology and transport properties, X-ray microtomography coupled with image analysis was used to characterize the 3D porous structure of activated carbons packed beds. Two different tube-to-particle ratios were investigated by changing the filter diameter. Polydispersed commercial granular activated carbon with mean particle size close to 1 mm was used. Specifically dedicated image analysis algorithms were developed to determine the total porosity, the pore size distribution, and the radial porosity profiles. For both filter diameters, the total porosity measured by image analysis was very close to the value determined ‘physically’ knowing the carbon mass, its bulk density and the dimension of the filter. The comparison of the pore size distributions indicates that void sizes are almost normally distributed around only one maximum for the large filter, while the distribution is larger and presents a more complex shape in the small filter. The radial porosity profiles showed an increase of the porosity from the center of the filter to the wall accompanied with an oscillatory behaviour at the small scale. A deeper analysis based on the power spectrum indicated a periodic behaviour in the large filter, with a characteristic length matching well with the carbon particle size: the carbon grains are uniformly packed layer by layer in the bed. In the small filter, oscillations were found to be not periodic suggesting an uneven packing of grains.*

**Keywords** X-ray microtomography, activated carbon, 3D packing structure, void distribution

### 1 INTRODUCTION

Activated carbon packed bed filters are commonly used to remove contaminants from gas streams, e.g. for flue gas treatment or respiratory protection. When the gas is forced through the filter, the pollutant is adsorbed on the activated carbon. The filter progressively saturates from the top to the bottom until breakthrough occurs, corresponding to the maximum life time of the filter. The so-called breakthrough curve is the plot of the vapour/gas concentration at the outlet of the bed, relative to the actual concentration at the inlet, as a function of time. If separation only results from physisorption and if the experiments are performed under constant inlet vapour concentration and superficial velocity, the shape and the width of the obtained breakthrough curve gives an indication of the bed efficiency: a sharper curve being an indication of a more efficient removal process. The shape of the breakthrough curve reflects how the concentration front moves through the bed, which depends roughly on two factors: the texture of the adsorbent at the nanometric scale and the macroscopic transport process in the bed. The textural characteristics of the adsorbent such as its pore volume, specific surface area and pore size distribution, can be accurately determined, e.g. from the analysis of the nitrogen adsorption isotherms at 77 K. On the other hand, the size and geometry of the bed and the adsorbent particles, which determine the transport properties within the bed, can be chosen at the time of the filter design. However, once the adsorbent is chosen in function of its texture and the filter is designed, other factors can influence the movement of the concentration front, making it more dispersive (i.e. a less sharp breakthrough curve). Indeed, when adsorbent particles are randomly packed in a bed, the void fraction in the bed and the spatial distribution of the adsorbent particles in the bed, which are determining factors for the transport properties, can only be calculated approximately. Moreover, wall effects can lead to a maldistribution of adsorbent particles (Suzuki et al. 2008) which can greatly modify the shape of the concentration front inside the bed. Hence, the possibility to characterize the 3D structure of activated carbon beds by X-ray microtomography will greatly help in understanding of

the macroscopic transport mechanisms and consequently help to develop more efficient devices for vapour/gas separation by adsorption processes.

In this work, X-ray microtomography coupled to image analysis is used to determine the void fraction and the void size distribution in the two beds as well as the radial porosity profiles. This technique has been recently used to determine axial and radial concentration profiles during dynamic adsorption experiments (Léonard et al. 2008; Lodewyckx et al. 2006)

## 2 MATERIALS AND METHODS

### 2.1. Activated carbon filters

Two kind of plastic canisters with the same length (33 mm) and different diameters were used in this study: FG (diameter = 26 mm) and fp (diameter = 15 mm). They were filled (7 g for FG and 2 g for fp) with a polydispersed commercial granular activated carbon, Chemviron Carbon BPL, whose properties are indicated in Table 1. Each filter was scanned in the X-ray microtomograph in order to determine their 3D structure.

Table 1. Properties of the BPL carbon

Mean particle diameter	1 mm
BET specific surface area	$1011 \text{ m}^2 \text{ g}^{-1}$
Dubinin-Radushkevich micropore volume	$0.36 \text{ cm}^3 \text{ g}^{-1}$
Characteristic energy of adsorption	$22.7 \text{ J mol}^{-1}$

### 2.2. X-ray microtomograph

The X-ray microtomographic device used was a “Skyscan-1074 X-ray scanner” (Skyscan, Kontich, Belgium). The cone-beam source operated at 40 kV and 1 mA. The detector was a 2D, 768 pixels  $\times$  576 pixels, 8-bit X-ray camera with a spatial resolution of 41  $\mu\text{m}$ . The rotation step was fixed at the minimum, 0.9°, in order to improve image quality, giving total acquisition times close to 10 minutes. For each filter, a Feldkamp type algorithm was used to reconstruct about 500 cross sections images separated by 41  $\mu\text{m}$  (Figure 1a and 1b). The 3D images were built by stacking the cross section images (Figure 1c).

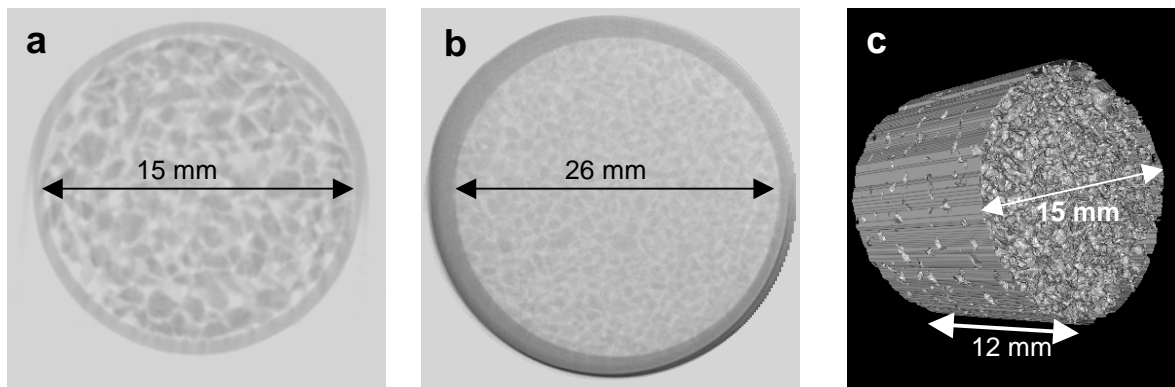


Figure 1: Typical transversal sections of: a) fp and b) FG virgin beds; c) 3D reconstruction of the fp virgin bed

### 2.3. Image analysis

X-ray microtomography provides a set of grey tone cross section images of the bed in which each grey tone is determined by the X-ray attenuation coefficient of the various points of the structure. The 3D image of a bed is formed by two phases: the carbon grains at low grey levels (dark voxels) and the void space between the grains at high grey levels (bright voxels). To determine the void fraction and the size distribution of voids, the 3D image of the bed must first be segmented. This operation allows determining which phase each voxel of the 3D image belongs to. Figures 1a and b present a non-homogeneous lighting in which the carbon grains placed near the walls of the bed are brighter than those placed nearest the centre. To correct this wall effect a “white-top-hat” (WTH) operator was applied on the 3D image (Soille 1999). This operator extracts “white” structures smaller than a given

size, i.e., structures that do not contain a specified structuring element (SE) which in our case was a sphere (approximated by an octahedron) with a size of 10 voxels. The resulting image was afterwards binarised by assigning a value of 1 to all voxels with an intensity below a given threshold (carbon grains) and a value of 0 to the others (background). Practically, the optimum threshold was easily determined manually using the histogram of grey levels of the image.

From the 3D processed binary images, the void fraction ( $\delta_{image}$ ), defined as the fraction of voxels of the image that belongs to the voids between the carbon grains, was measured first. As the carbon beds present a continuous and rather disordered void structure, a standard granulometric measurement could not be applied. Then, to quantify the void size distribution, the opening size distribution (Soille1999) was calculated. This method allows assigning a size to both continuous and individual particles. When an opening transformation is performed on a binary image with a SE of size  $\lambda$ , the image was replaced by the envelope of all SEs inscribed in its objects. For the sake of simplicity, spheres of increasing radii  $\lambda$  (approximated by an octahedron) were used. When an image was opened by a sphere whose diameter was smaller than the smallest features of its objects, it remained unchanged. As the size of the sphere increased, larger parts of the objects were removed by the opening transformation. Therefore, opening could be considered as equivalent to a physical sieving process.

Radial profiles were determined as follows: the sum of the grey-level intensity of all voxels within a layer located at a distance  $r$  of the centre of the sample is normalized by the number of voxels in the layer. These mean intensities are then drawn in function of  $r$ . For this kind of measurements the shape of the layers must be chosen in function of the structure of the sample. In our case, considering the geometry of the beds, layers were defined by the volume in between successive cylinders. Radial profiles were built considering (a) the raw grey level of voids and (b) by assigning to them a grey level value equal to 0.

### 3 RESULTS

BPL commercial carbon grains of 1 mm mean diameter were randomly packed in fp and FG filters. The void fraction measured by image analysis was  $\delta_{image} = 0.35$  and 0.30 respectively. Those values are very close and agree well with the void fractions  $\delta_p = 0.32$  and 0.26 determined physically using the following expression:

$$\delta_p = 1 - \frac{M}{\rho \cdot V} \quad (1)$$

where  $M$  is the weight or carbon in the bed,  $\rho$  is the bulk density of BPL carbon, and  $V$  is the volume of the packed bed, considered as a cylinder.

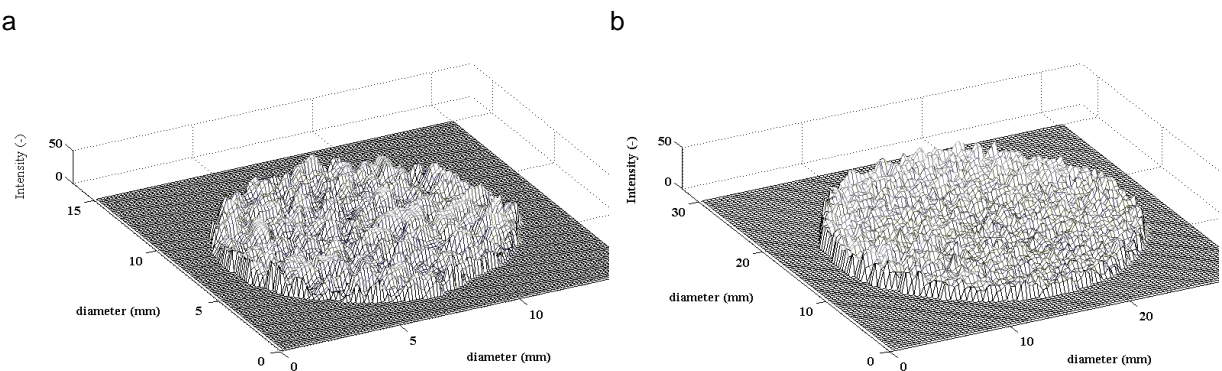


Figure 2: Grey level intensity distribution with a cross section image for: a) fp and b) FG

A simple observation of the 2D (Figures 1a and b) suggests that voids distribute differently in the two beds. This can also be seen on Figure 2a and b representing the distribution of grey levels within a cross section of the small and large beds, respectively. Valleys correspond to carbon grains (low grey levels) while peaks correspond to interstitial voids (high grey levels). The pattern is obviously smoother in the case of the large filter. This is confirmed by the void size distributions obtained from the segmented 3D images. Figure 3 indicates that for FG, void sizes are almost normally distributed

around only one maximum (FG mean void size =  $0.38 \pm 0.09$  mm) whereas for fp the distribution is larger and presents a more complex shape (fp mean void size =  $0.50 \pm 0.12$  mm). This indicates that in fp there exist local variations of interparticle spaces that certainly will affect the gas flow through the bed.

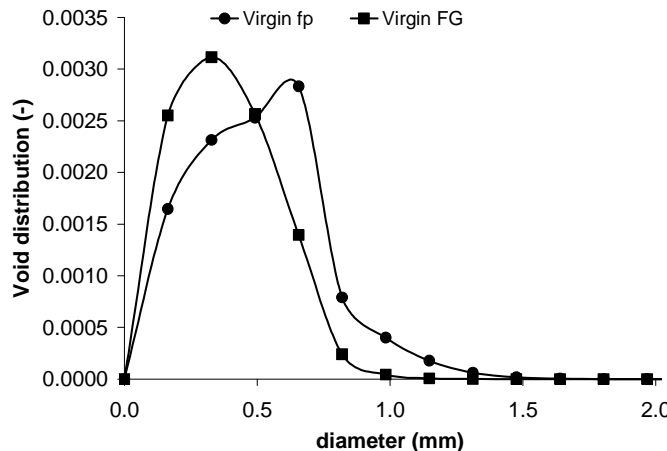


Figure 3: 3D void size distributions

Radial profiles (Figure 4) give information about the spatial distribution of the carbon grains in the two beds. Intensities (y-axis) are given in arbitrary units as only the variation of the grey tone intensity of images in function of the radius of the beds is relevant for our study. They show two main characteristics: i) the grey level intensity decreases from the external wall to the centre of the bed ii) this decrease is accompanied by an oscillatory behaviour at a small scale. The first characteristic is directly linked to the presence of the wall and indicates that the carbon grains concentration increases towards the centre of the bed. The higher porosity near the wall is well known for the preferential channelling it may induce (Winterberg et al. 2000). The second one has been described by several authors. In a packed bed of monodisperse particles, the radial void distribution undergoes damped oscillations reaching a constant value at some distance from the external wall, provided the ratio  $D/d_p$  is sufficiently high. At low  $D/d_p$ , this limiting value may never be reached, indicating that the medium is anisotropic (Negrini et al. 1999; Suzuki, Shimura, Iimura, & Hirota 2008).

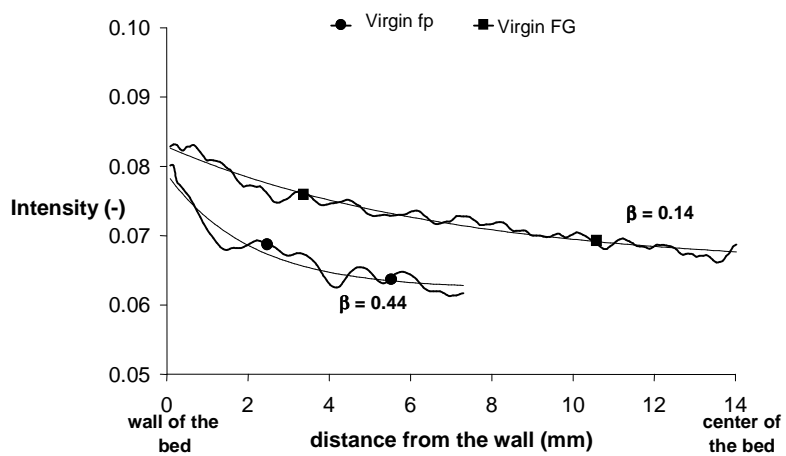


Figure 4: Radial void distributions

To quantify the influence of the filter diameter on this wall effect, radial measurements were fitted according to the monotonic exponential

$$I_{decay}(r, \mu) = A(\mu) + B(\mu)e^{(-\beta r)} \quad (2)$$

where  $I_{decay}$  is the fitted grey level intensity,  $\beta$  is the decay constant which depends of the tube-to-particle-diameter ratio,  $D/d$ , where  $D$  and  $d$  are the diameters of the canister and of the carbon grains respectively, and  $0 < r < D/2$ .  $A$  and  $B$  are parameters that depend of the attenuation coefficient of the

adsorbent. The measured and the fitted radial profiles are shown in Figure 4 as well as the obtained  $\beta$  values. In both cases the correlation coefficient was larger than 0.98. For the activated carbon used in this study it was found that  $A = 0.062$  and  $B = 0.016$ . The larger decay constant for fp ( $\beta = 0.44$ ) than for FG ( $\beta = 0.14$ ) indicates that, in the smaller canister, carbon grains are less uniformly distributed with a larger gradient of concentration from the walls to the centre of the bed. For the small canister, a constant value of porosity has not been reached in the centre, while stabilisation could be nearly assumed for the large filter.

To analyse the oscillating behaviour, the fitted radial profiles  $I_{decay}(r)$  were subtracted from the measured ones, i.e.

$$I_{osc}(r) = I(r) - I_{decay}(r) \quad (3)$$

Figure 5 shows that for FG, oscillations are almost periodic, with valleys and peaks. This is confirmed by the power spectrum of  $I_{osc}$  (Figure 6) which presents a main peak, at the frequency  $\omega = 7.12 \text{ mm}^{-1}$ , and its harmonics. This value is related to the characteristic length  $\lambda = 2\pi/\omega = 0.8 \text{ mm}$  which matches well with the diameter of a carbon grain and confirms that carbon grains are uniformly packed layer by layer in the bed. On the contrary, for fp oscillations are not periodic suggesting an uneven packing of grains. Moreover, in this case it is not relevant to calculate a characteristic length from a power spectrum because  $I_{osc}$  is a short set with not enough oscillations to detect a clear periodicity.

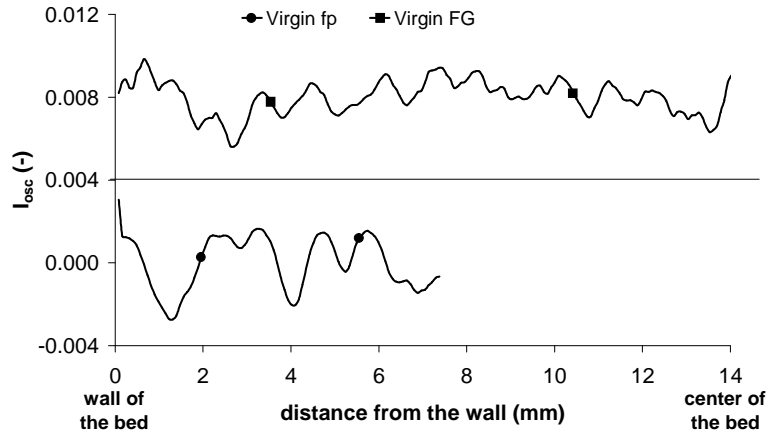


Figure 5: Intensity oscillations for FG and fp

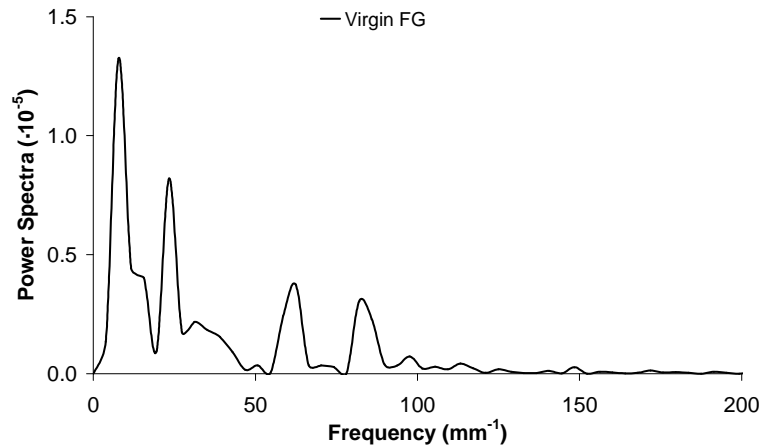


Figure 6: Power spectrum of  $I_{osc}$  for FG

## 4 DISCUSSION

The void fraction and its distribution in a packed bed have a direct impact on the fluid/particles hydrodynamics interactions. The efficiency of catalytic fixed-bed reactors or adsorbers can be greatly affected by the transport properties. The knowledge of the void distribution inside a bed is very important to set up models allowing the simulation of local velocity profiles, for example. However, its experimental determination was difficult until the development of non-destructive investigating methods such as X-ray tomography (Toye et al. 1998). X-ray  $\mu$ -tomography enabled us to visualise the structure of the adsorbent bed and the 3D  $\mu$ -tomograms were analysed to determine the spatial distribution of voids in the bed.

To illustrate the potential of this technique, two beds with different diameters randomly filled with a commercial active carbon were scanned by X-ray  $\mu$ -tomography. Each reconstructed 3D image was processed to determine the total porosity and the void size distribution. Taking into account that each 3D image is formed by piling approximately 500 2D images, it must be pointed out that image processing and measurements require powerful computer resources to avoid time consuming calculations. In order to discriminate between pixels belonging to the carbon grains and to the voids, images were first pre-processed to enhance the contrast.

Radial profiles (Figure 4) showed that void fraction is characterized by an oscillating behaviour. This periodic behaviour is characteristic of randomly packed beds in which walls exert an effect of confinement on the localization of the particles, which tends to organise them in more ordered layers near the wall (Sita Ram Rao 1994; Suzuki, Shimura, Iimura, & Hirota 2008). Oscillations are superimposed to an exponential decay of the grey level intensity when going from the wall to the centre of the tube. This indicates that carbon grains tend to assemble in the centre of the bed. The extent of this wall effect depends on the  $D/d$  ratio and of the polydispersity of carbon grains (Kwapinski et al. 2004). A comparison between radial profiles of the two studied packed beds (Figure 4), showed that, as one could expect, wall effects are less marked in the large canister, which presents a smaller void fraction, a narrow void size distribution and a more ordered spatial distribution of grains. Indeed, for the FG, the decay coefficient in equation 2, which only depends on  $D/d_p$ , is smaller than for  $f_p$ . This results in a more flat radial profile. Moreover, the power spectra (Figure 5) of the periodic component put in evidence a characteristic length which agrees with the diameter of a carbon grain ( $\sim 1\text{mm}$ ).

## 5 CONCLUSIONS

X-ray micro-tomography coupled with image analysis was used to characterize the 3D microstructure of BPL active carbon beds. It was shown that this methodology is a powerful tool to determine the void fraction and its distribution in a non-destructive way. The results confirmed the influence of the tube-to-particle ratio on the structural properties of activated carbon beds. In further works other parameters such as tortuosity and connectivity will be analysed. The characteristics of the bed microstructure will be linked with the motion of an adsorbate concentration front in the carbon filter. Finally, the 3D images will be used to simulate the filter operation by the lattice Boltzmann methodology, taking into account the coupling between gas flow pattern and adsorption.

## 6 ACKNOWLEDGEMENTS

M.C.A.A. acknowledges financial support of MEC and FICYT as a postdoctoral contract. A. Léonard is grateful to the Fund for Scientific Research (FRS-FNRS, Belgium) for a Research Associate Position.

## 7 REFERENCES

KWAPINSKI, W., WINTERBERG, M., TSOTSAS, E., MEWES, D., (2004), Experimental and Theoretical Investigation of Concentration and Temperature Profiles in a Narrow Packed Bed Adsorber, *Chemical Engineering and Technology*, 27, pp. 1179-1186.

LÉONARD, A., WULLENS, H., BLACHER, S., MARCHOT, P., TOYE, D., CRINE, M., LODEWYCKX, P., (2008), In situ observation of wall effects in activated carbon filters by x-ray microtomography, *Separation and Purification Technology*, In Press, Accepted Manuscript.

LODEWYCKX, P., BLACHER, S., LÉONARD, A., (2006), Use of x-ray microtomography to visualise dynamic adsorption of organic vapour and water vapour on activated carbon, *Adsorption*, 12, pp. 19-26.

NEGRINI, A.L., FUELBER, A., FREIRE, J.T., THOMÉO, J.C., (1999), Fluid dynamics of air in a packed bed: velocity profiles and the continuum model assumption, *Brazilian Journal of Chemical Engineering*, 16, 4, pp. 421-432.

SITA RAM RAO, K.V. 1994, *Wall effects in packed beds*, PhD Thesis, Indian Institute of Science, Bangalore, India.

SOILLE, P., (1999), *Morphological Image Analysis – Principles and Applications* Springer-Verlag, New York.

SUZUKI, M., SHINMURA, T., IIMURA, K., HIROTA, M., (2008), *Study of Wall Effect on Particle Packing Structure using X-ray Micro Computed Tomography*, In Proc: 5th World Congress on Industrial Process Tomography, Bergen, Norway, 2007, pp. 304-311.

TOYE, D., MARCHOT, P., CRINE, M., PELSSER, A.-M., L'HOMME, G., (1998), Local measurements of void fraction and liquid holdup in packed columns using X-ray computed tomography , *Chemical Engineering and Processing*, 37, 6, pp. 511-520.

WINTERBERG, M. AND TSOTSAS, E., (2000), Impact of tube-to-particle-diameter ratio on pressure drops in packed beds, *AIChE J.*, 46, 5, pp. 1084-1088.